A Journal of the Gesellschaft Deutscher Chemiker

Angewandte International Edition

GDCh

Chemie

www.angewandte.org

Accepted Article

Title: Harvesting Hydrogen Bond Network: Enhance the Anti-Solvatochromic Two-Photon Fluorescence for Cirrhosis Imaging

Authors: Tianbing Ren, Wang Xu, Qianling Zhang, Xingxing Zhang, Siyu Wen, Haibo Yi, Lin Yuan, and Xiaobing Zhang

To be cited as: *Angew. Chem. Int. Ed.* 10.1002/anie.201800293
Angew. Chem. 10.1002/ange.201800293

Link to VoR: http://dx.doi.org/10.1002/anie.201800293
http://dx.doi.org/10.1002/ange.201800293

WILEY-VCH

10.1002/anie.201800293

WILEY-VCH

Harvesting Hydrogen Bond Network: Enhance the Anti-Solvatochromic Two-Photon Fluorescence for Cirrhosis Imaging

Tian-Bing Ren, Wang Xu, Qian-Ling Zhang, Xing-Xing Zhang, Si-Yu Wen, Hai-Bo Yi, Lin Yuan* and Xiao-Bing Zhang

Abstract: Two-photon imaging is an emerging tool for biomedical research and clinical diagnostics. Electron donor–acceptor (D–A) type molecules are the most widely employed two-photon scaffolds. However, current D–A type fluorophores suffer from solvatochromic quenching in aqueous biological samples. To address this issue, we devised a novel class of D-A type GFP chromophore analogues that form hydrogen bond network in water to improve the two-photon efficiency. Our design results in **TPC** dyes with 0.80 quantum yield and large two-photon cross section (210 GM) in water. This strategy to harvest hydrogen bonds can be generalized to design two-photon materials with anti-solvatochromic fluorescence. To demonstrate the improved *in vivo* imaging, we designed a sulfide probe based on **TPC** dyes and monitored endogenous H_2S generation and scavenging in the cirrhotic rat liver for the first time.

Molecular imaging has revolutionized biomedical research and clinical diagnostics.[1] Among the great diversity of imaging techniques, two-photon fluorescence imaging stands out due to its non-invasiveness and deep tissue penetration.[2] Particularly, electron donor–acceptor (D–A) type molecules are the most commonly adopted two-photon scaffolds due to their large absorbance coefficients and redshifted emission.[3] However, in protic polar solvents, D-A type molecules usually suffer from fluorescence quenching with bathochromic shifts, known as solvatochromism.[3b,4] Although this phenomenon was proven useful in polarity sensing,[5] the poor quantum yields of D-A type molecules under physiological condition inevitably hamper their applications *in vivo*.[6] There remains an urgent need to design D-A type two-photon fluorophores with minimized quenching in water and robust performance in biological research.[4a]

Physically, solvatochromism is manifested as emission redshift and fluorescence quenching, both originate from the polar interactions between the electronic structure and the solvent.[7] Redshift is due to matching alignment between the molecules and the solvent that lowers the HOMO-LUMO gap.[8] Quenching is more complicated and influenced by many factors. For instance, twisted intramolecular charge transfer (TICT) dissipates the excitation energy through bond rotation (Figure 1A).[9] "Energy gap law" releases energy through electron transition from excited states to the empty orbitals.[10] Excited state proton transfer mostly occurs in protic polar solvents, where protons migrate from solvents to the fluorophores and quench the excited electrons (Figure 1A).[11] On the other hand, D-A type fluorophores rely on intramolecular charge transfer (ICT) for bright emission.[12] The fluorescence properties might be jeopardized if the D-A group were overly truncated. Given all the complexities, a thorough evaluation is necessary to design new D-A type fluorophores.

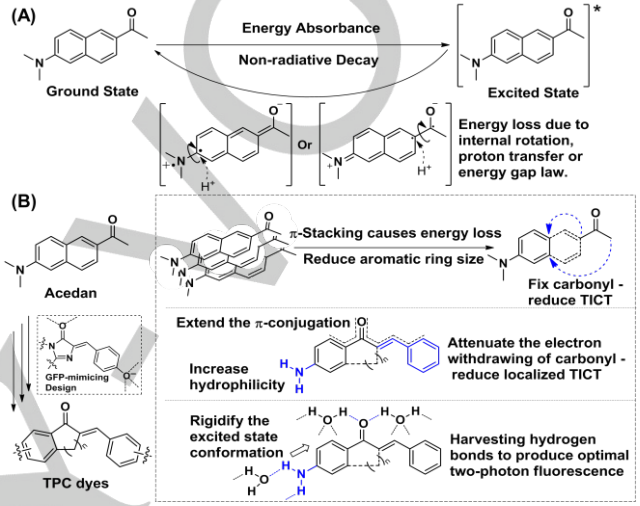

Figure 1. (A) The quenching mechanisms of traditional D-A type fluorophores (dimethylamino acedan). (B) General design strategy of new D-A type **TPC** (two-photon chalcone) dyes.

Our design is inspired by a natural D-A type molecule, the GFP chromophore,[13] which shows three features: 1) reduced aggregation and non-radiative decay from the small aromatic scaffold;[14] 2) attenuated quenching by restrained donor/acceptor; 3) most remarkably, a hydrogen bond network (HBN) that modulates the emission profile. Inside the protein pocket, GFP chromophore is surrounded by HBN that stabilizes the electronic states, minimizes the energy dissipation and strengthens ICT (Figure 1B).[15] It is noteworthy that most fluorophores are quenched by hydrogen bonds, with GFP chromophore being an exception only in the protein pocket.[11] Our design aims at incorporating all the three features of GFP chromophore with an emphasis on harvesting hydrogen bonds in the open solvent environment.

By replacing the dihydroimidazole ring of GFP chromophore with cyclopentanone appended on dimethylaminobenzene, we developed a simple and facile scheme to produce **TPC** dyes by one-step nucleophilic substitution with indanones and benzaldehydes under mild conditions (Scheme S1). As a proof-of-concept, we synthesized three **TPC** dyes by altering the substituents on the 3-position of ring A (Figure 2A). Their emission spectra in different solvents were measured together with three known D-A type two-photon dyes, **Acedan-NH$_2$**, **Ans** and **Naph-NH$_2$** (Figures 2B, S1). The known D-A type fluorophores exhibit substantial solvatochromism, quenching in protic polar media (Figures 2B, S2a-2c, S2g-h). In comparison, all **TPC** dyes exhibit anti-solvatochromic fluorescence emission. **TPC1** displays gradual quantum yield increment with solvent polarity, changing from Φ_f = 0.16 in DCM (λ_{max} 482 nm) to 0.23 in MeCN (λ_{max} 506 nm) and 0.30 in ethanol (λ_{max} 508 nm)

[*] T.-B. Ren,[▽] Dr. W. Xu,[▽] Q.-L. Zhang, X.-X. Zhang, S.-Y. Wen, Dr. H.-B. Yi, Prof. Dr. L. Yuan, Prof. Dr. X.- B. Zhang
State Key Laboratory of Chemo/Biosensing and Chemometrics, College of Chemistry and Chemical Engineering
Hunan University
Changsha 410082 (PR China)
E-mail: lyuan@hnu.edu.cn
[▽]These authors contributed equally
Supporting information for this article is given via a link at the end of the document.

(Table S1). However, in PBS buffer the quantum yield drops to less than 0.02. The dimethylamino group is likely too hydrophobic and electron-donating, thus not only reduces the water solubility of **TPC1** (Figure S3), but also counters our design to reduce TICT. By altering the dimethylamino group, we produced more hydrophilic **TPC2** and **TPC3**, both emitting stronger in PBS buffer (Figure S2e-2f). **TPC3** exhibits the most remarkable anti-solvatochromic fluorescence (quantum yields in PBS (0.80) > EtOH (0.53) > MeCN (0.12) > DCM (0.02)), 113-time stronger emission in PBS than in DCM (Figure S2f). Under UV irradiation, **TPC3** exhibits clear fluorescence turn-on with increasing PBS ratio (Figures 2C, S4a), contrasting the quenching of **Acedan-NH$_2$** (Figures 2D, S4b). Fluorescence lifetime also exhibit anti-solvatochromic pattern: as the solvent polarity increases, the lifetime of **TPC3** significantly extends (Table S2 & Figures S5).

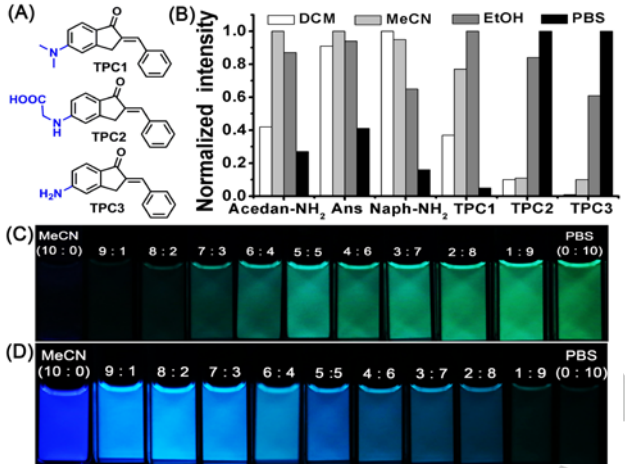

Figure 2. (A) Structures of **TPC1-3**. (B) Normalized fluorescence intensities of **Acedan-NH$_2$**, **Ans, Naph-NH$_2$**, and **TPC1-3** (5 μM) in different solvents. (C) and (D) Fluorescent photographs of **TPC3** and **Acedan-NH$_2$** (5 μM) in MeCN-PBS buffer mixtures under 365 nm excitation.

DFT calculations indicate that HOMO distribute on ring A of **TPC3**, whereas LUMO cover ring B (Figure S6). We hypothesize that HOMO determines the solvatochromism whereas modifications on ring B lead to adjustment of emission wavelengths. The calculations suggest that 5-, 7-, and 9-positions of **TPC3** have denser LUMO electrons. Thus we synthesized a series of **TPC** dyes with their 5- and 7-positions modified by electron donors or acceptors. Fluorescence spectra comparison between **TPC4**-**TPC5** and **TPC6**-**TPC7** indicates that both weak electron donors and acceptors redshift the emission maxima (Figure S7A-D & Table 1). However, **TPC4** and **TPC6** are not completely anti-solvatochromic because the strong electron donor - methoxy group pushes HOMO to ring B (Figure S6). To confirm the assumption, we synthesized **C1** with 7-dimethylamino and compared its spectra with **TPC6**. On **TPC6**, the HOMO still mainly rests on ring A, whereas in **C1** the HOMO shifts to ring B (Figure S8), thus becoming solvatochromic (Figure S9a-10a**)**. Similar observation was seen on **C2** (Figures S8, S9b-S10b). The HOMO migrates further to ring B, making **C2** even more solvatochromic. Thus weak electron acceptors on ring B can redshift the emission of **TPC** dyes while maintaining their anti-solvatochromic fluorescence.

Regioisomeric comparison was conducted between **TPC5** and **TPC7**. Both molecules exhibit anti-solvatochromic fluorescence, but the bulky 5-COOH on **TPC5** hampers the overall conjugation, making it less redshifted than **TPC7**. **TPC8**, equipped with 7-cyanide, clearly emits anti-solvatochromic fluorescence (Figure S7 and Table 1). We hence confirm that by modifying ring B with acceptors at less sterically hindered positions, slight emission tuning can be achieved without compromising the anti-solvatochromic fluorescence. **TPC9** and **TPC10** replaced the benzene ring B with electron deficient pyridine. Both dyes showed substantial redshift, further confirming our hypothesis. **TPC11** and **TPC12** changed the cyclopentanone linker between ring A and ring B to dihydrofuranone and cyclohexanone, affecting the planar conjugation and reducing their quantum yields (Table 1). As revealed by DFT calculations, ring B of **TPC12** forms an angle of 149.24° at cyclohexanone (Figure S11). **C3** has flexible connection between ring A and B, hence showing negligible emission in all solvents (Table 1). In total, structure tuning on ring B resulted in emission wavelengths adjustment.

Table 1. Chemical structures and optical properties of **TPC** dyes.

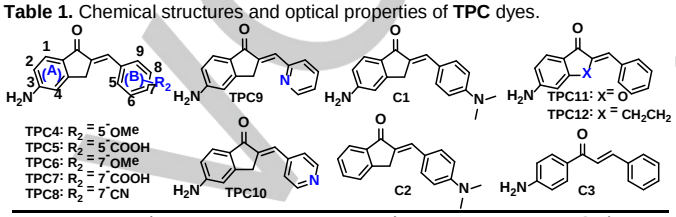

Dye	λ_{Abs} /nm	ε($M^{-1}cm^{-1}$)	λ_{Em} /nm	Φ[a]	Stokes shift/nm
TPC3	375	43400	498	0.80	123
TPC4	381	34400	501	0.34	120
TPC5	374	8010	503	0.39	129
TPC6	388	10200	493	0.20	105
TPC7	382	6200	518	0.49	136
TPC8	388	9800	535	0.17	147
TPC9	381	36000	522	0.52	141
TPC10	383	37200	535	0.29	152
TPC11	363	19000	505	0.13	142
TPC12	378	18200	528	0.072	150
C1	426	9020	572	0.004	146
C2	445	7440	524	/	79
C3	344	14400	/	/	/

[a]The quantum yields were determined using fluorescein as reference (Φ_f = 0.95 in 0.1 M NaOH solution).

To elaborate the functions of HBN in improving the fluorescence of **TPC** dyes, we conducted a series of simulations. We hypothesize that the HBN functions in three ways: 1) it restrains the internal rotation, thus reducing the non-radiative dissipation; 2) it helps dissolve the molecules in protic polar solvents; 3) it facilitates and stabilizes the ICT states that lead to redshifts. These assumptions were confirmed by energy comparisons between solvated and non-solvated **TPC3**. In Figure 3A, S_1-min and S_1-max are the lowest and highest energy excited states of **TPC3**. S_1-min has a nearly planar conformation with 0-degree dihedral angle between ring A and B, whereas S_1-max exhibits 90-degree dihedral angle (Figure S12a). The excited state energy increases with the dihedral angle and solvent polarity (Figure S12b). The calculated oscillator strengths reveal that in polar solvents, **TPC3** presents higher chance to absorb or emit light than in non-polar solvent (Figure S12c).

On **TPC3** structure, there are two exposed heteroatoms that can form hydrogen bonds with solvents: the carbonyl group of the cyclopentanone and the amino group on ring A. In the simulated environment of MeCN-water mixture, we tested hydrogen bonding on both positions (Figure 3A and S13A). Apparently, the change of rotation barrier and oscillator strength is associated with the change of hydrogen bonds (Figure 3B and S13B). The ability of molecules undergoing electronic state transition is manifested by the difference of oscillator strengths at 0 degree and 90 degree dihedral angles. More hydrogen

10.1002/anie.201800293

bonds prompt smaller depth, hence the molecule is easier to absorb and emit energy (Figure 3B). In addition, we postulate that the HBN shapes the molecule in a maximally fluorescent state by limiting vibrational and rotational energy loss. This phenomenon can be named *hydrogen bond induced enhanced emission (HIEE)*. In addition, dynamic light scattering indicates that **TPC3** remains solvated in the water-MeCN mixture. Hence its quantum yield increase originates from the interactions with water molecules, not through aggregation-induced emission (Figure S14).

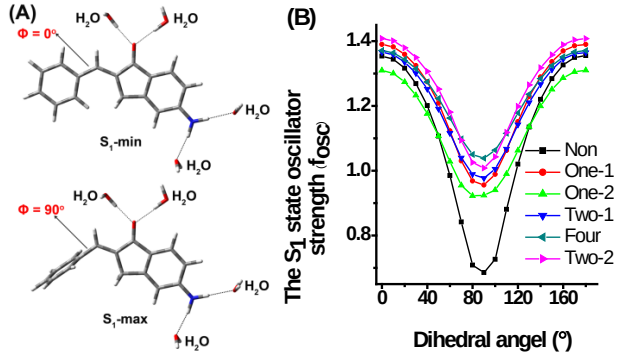

Figure 3. (A) S_1-min and S_1-max conformations of **TPC3** in the first excited state with hydrogen bonds attached to either carbonyl or amino group. (B) The oscillator strength of S_1 excited state of **TPC3** with different numbers of hydrogen bonds (None to four). Both metrics were plotted with increasing twist angles (φ) at the bridging bond of ring B. The simulation is conducted in the mixture of MeCN and water.

We next conducted a series of studies on the selected molecule **TPC3** and proved that its excellent two-photon performance, chemical stability and photo-stability is suitable for biological studies (Figure S15-20). By engineering the 3-amino group of **TPC3** with azide, we altered its electronic structure and generated **TPC-N$_3$** (Figure 4). **TPC-N$_3$** itself exhibits negligible fluorescence emission under UV; upon reaction with hydrogen sulfide (H_2S), the azide is reduced to amino, yielding **TPC3** and recovering the emission (Scheme S2). **TPC-N$_3$** can thus serve as a potent two-photon fluorescent probe for sulfide in the biological systems.

Endogenous H_2S plays an essential role in antagonizing chronic liver injury or cirrhosis by mediating vasodilation and increasing hepatic arterial buffer responses.[16] Internally, H_2S level is modulated by cystathionine γ lyase (CSE). However, there is no direct evaluation of the H_2S dynamics during cirrhosis due to the lack of potent sensing tools. To tackle this issue, we first proved that **TPC-N$_3$** could selectively monitor endogenous sulfide generation both *in vitro* and *in vivo* (Figure S21-24). The penetration depth of **TPC-N$_3$** can reach 100 μm in the liver tissue (Figure S25).

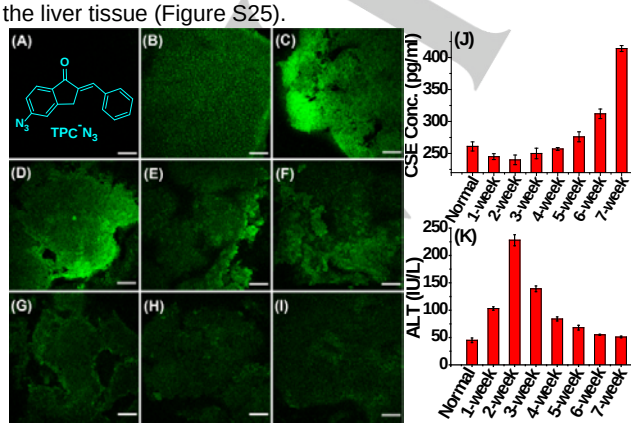

Figure 4. Two-photon imaging of **TPC-N$_3$** (10 μM) in liver tissue of cirrhotic mice: (A) Normal mice liver tissue only; (B) Normal mice liver tissue with **TPC-N$_3$**, (C)-(I) mice with CCl_4 treatment after 1 to 7 weeks, liver tissue extracted then incubated with **TPC-N$_3$**. Excitation: 810 nm. Emission: 500-560 nm. Scale bar: 150 μm. (J) Quantification of cystathionine γ lyase (CSE) levels in normal and cirrhosis liver tissue by ELISA. (K) Serum ALT levels in normal and cirrhosis mice.

To build a reliable cirrhosis model, mice were subcutaneously injected with CCl_4 to induce hepatotoxicity on a daily level for over 7 weeks. The liver tissue was harvested at different time points and stained with **TPC-N$_3$**. Two-photon imaging clearly indicated a sharp purge of H_2S in liver upon first week of treatment (Figure 4A-I and S27a). Comparing to normal liver, the fluorescence intensity increased over three-fold (Figure S27a). Reports showed that to antagonize acute liver injury, endogenous H_2S was abundantly produced and consumed as an internal gasotransmitter.[17] In addition, quantitation of key enzymes expressed by hepatocytes, such as aspartate transaminase (AST) and alanine transaminase (ALT) saw their increased expression levels (Figure 4K and S27b), indicating liver self-remediation.[18] Interestingly, with the progression of liver injury, H_2S level significantly dropped (Figure 4A-I, Figure S27a). Immunoassay reveals that CSE level in liver tissue initially decreased, followed by increase and a final purge at week 7 (Figure 4J). This indicates that liver CSE is heavily expressed to compensate for H_2S depletion. The ALT and AST levels also stepped down after the initial increase, reaching normal levels (Figure 4K and S27b). This proved that liver injury has entered late stage and hepatocytes can no longer support the liver self-repairing, resulting in cirrhosis (Figure S26 and S27).[19] Hematoxylin and eosin stain clearly showed fibrotic bands and distortion of the liver tissue (Figure S27c). This is the first direct visualization of H_2S generation and consumption in a liver cirrhosis model. The probe provides a sensitive and powerful tool to study chronic liver diseases.

In conclusion, a new series of D-A type GFP chromophore analogues (**TPC** dyes) that can harvest hydrogen bonds in water to induce strong anti-solvatochromic fluorescence was devised. Such a feature makes **TPC** dyes especially attractive for two-photon molecular imaging in the biological specimens. Mechanism and structure-activity studies elaborated that **TPC** dyes bind to water molecules through multiple hydrogen bonds, achieving better solubility and higher stability of the ICT excited states. Such an unprecedented design strategy utilizing HBN can potentially be generalized to the pursuit of two-photon fluorophores with strong fluorescence in aqueous environment. To demonstrate their biological applications, we synthesized a H_2S selective probe based on **TPC** scaffold and for the first time visualized H_2S generation and consumption in the cirrhotic liver tissue.

Acknowledgements

This work is supported by NSFC (21622504, 21735001, 21521063), the Science and Technology Project of Hunan Province (2017RS3019). We are grateful to Prof. Peng Wu from Sichuan University for measuring the fluorescence lifetime data.

Keywords: fluorescent dyes • hydrogen bond network • anti-solvatochromism • two-photon • cirrhosis

[1] a) X. Chen, F. Wang, J. Y. Hyun, T. Wei, J. Qiang, X. Ren, I. Shin, J. Yoon, *Chem. Soc. Rev.* **2016**, *45*, 2976-3016; b) A. T. Aron, K. M. Ramos-Torres, J. A. Cotruvo, C. J. Chang, *Acc. Chem. Res.* **2015**, *48*, 2434-2442; c) Z. Yang, J. Cao, Y. He, J. H. Yang, T. Kim, X. Peng, J. S. Kim, *Chem. Soc. Rev.* **2014**, *43*, 4563-4601; d) Xu, W.; Zeng, Z.; Jiang, J. H.; Chang, Y. T.; Yuan. L. *Angew. Chem. Int. Ed.* **2016**, *55*, 13658-13699.

[2] H. M. Kim, B. R. Cho, *Chem. Rev.* **2015**, *115*, 5014-5055.

[3] a) D. Kim, H. Moon, S. H. Baik, S. Singha, Y. W. Jun, T. Wang, K. H. Kim, B. S. Park, J. Jung, I. Mook-Jung, K. H. Ahn, *J. Am. Chem. Soc.* **2015**, *137*, 6781-6789; b) T. Ren, W. Xu, F. Jin, D. Cheng, L. Zhang, L. Yuan, X. Zhang, *Anal. Chem.* **2017**, *89*, 11427-11434; c) E. D. Cosco, J. R. Caram, O. T. Bruns, D. Franke, R. A. Day, E. P. Farr, M. G. Bawendi, E. M. Sletten, *Angew. Chem. Int. Ed.* **2017**, *56*, 13126-13129;.

[4] a) S. Singha, D. Kim, B. Roy, S. Sambasivan, H. Moon, A. S. Rao, J. Y. Kim, T. Joo, J. W. Park, Y. M. Rhee, T. Wang, K. H. Kim, Y. H. Shin, J. Jung, K. H. Ahn, *Chem. Sci.* **2015**, *6*, 4335-4342; b) E. Kim, Y. Lee, S. Lee, S. B. Park, *Acc. Chem. Res.* **2015**, *48*, 538-547; c) E. Yamaguchi, C. Wang, A. Fukazawa, M. Taki, Y. Sato, T. Sasaki, M. Ueda, N. Sasaki, T. Higashiyama, S. Yamaguchi, *Angew. Chem. Int. Ed.* **2015**, *54*, 4539-4543.

[5] H. M. Kim, C. Jung, B. R. Kim, S. Y. Jung, J. H. Hong, Y. G. Ko, K. J. Lee, B. R. Cho, *Angew. Chem. Int. Ed.* **2007**, *46*, 3460-3463.

[6] a) Y. J. Gong, X. B. Zhang, G. J. Mao, L. Su, H. M. Meng, W. Tan, S. Feng, G. Zhang, *Chem. Sci.* **2016**, *7*, 2275-2285; b) M. Sun, K. Mullen, M. Yin, *Chem. Soc. Rev.* **2016**, *45*, 1513-1528.

[7] a) H. R. Naughton, C. J. Abelt, *J. Phys. Chem. B* **2013**, *117*, 3323-3327; b) J. Catalan, in *Handbook of Solvents (2 ed.)*, ChemTec Publishing, Oxford, **2014**, pp. 581-622.

[8] a) V. G. Machado, R. I. Stock, C. Reichardt, *Chem. Rev.* **2014**, *114*, 10429-10475; b) Y. Yang, D. Li, C. Li, Y. Liu, K. Jiang, *Spectrochim. Acta A.* **2017**, *187*, 68-74.

[9] a) X. Liu, Q. Qiao, W. Tian, W. Liu, J. Chen, M. J. Lang, Z. Xu, *J. Am. Chem. Soc.* **2016**, *138*, 6960-6963; b) J. B. Grimm, B. P. English, J. Chen, J. P. Slaughter, Z. Zhang, A. Revyakin, R. Patel, J. J. Macklin, D. Normanno, R. H. Singer, T. Lionnet, L. D. Lavis, *Nat. Meth.* **2015**, *12*, 244-250.

[10] a) A. O. Doroshenko, M. D. Bilokin, V. G. Pivovarenko, *J. Photoch. Photobio. A* **2004**, *163*, 95-102; b) R. Englman, J. Jortner, *Mol. Phys.* **1970**, *18*, 145-164.

[11] M. Staniforth, W. D. Quan, T. N. V. Karsili, L. A. Baker, R. K. O'Reilly, V. G. Stavros, *J. Phys. Chem. A* **2017**, *121*, 6357-6365.

[12] S. Lee, K. K. Y. Yuen, K. A. Jolliffe, J. Yoon, *Chem. Soc. Rev.* **2015**, *44*, 1749-1762.

[13] a) L. M. Oltrogge, S. G. Boxer, *ACS Central Sci.* **2015**, *1*, 148-156; b) M. Drobizhev, N. S. Makarov, S. E. Tillo, T. E. Hughes, A. Rebane, *Nat. Meth.* **2011**, *8*, 393-399.

[14] a) D. Zhai, W. Xu, L. Zhang, Y. T. Chang, *Chem. Soc. Rev.* **2014**, *43*, 2402-2411; b) J. Mei, N. L. C. Leung, R. T. K. Kwok, J. W. Y. Lam, B. Z. Tang, *Chem. Rev.* **2015**, *115*, 11718-11940.

[15] a) G. Cui, Z. Lan, W. Thiel, *J. Am. Chem. Soc.* **2012**, *134*, 1662-1672; b) Y. Li, T. Liu, H. Liu, M. Z. Tian, Y. Li, *Acc. Chem. Res.* **2014**, *47*, 1186-1198.

[16] J. L. Wallace, R. Wang, *Nat. Rev. Drug Discov.* **2015**, *14*, 329-345.

[17] S. Mani, W. Cao, L. Wu, R. Wang, *Nitric Oxide* **2014**, 41, 62-71.

[18] E. G. Giannini, R. Testa, V. Savarino, *Can. Med. Assoc. J.* **2005**, 172, 367-379.

[19] a) S. Fiorucci, E. Antonelli, A. Mencarelli, S. Orlandi, B. Renga, G. Rizzo, E. Distrutti, V. Shah, A. Morelli, *Hepatology* **2005**, 42, 539-548; b) N. Zhang, Y. Zheng, W. Chen, R. Li, L. Song, L. Xu, K. Xu, *J. Huazhong U. Sci-Med.* **2017**, 37, 705-710.

10.1002/anie.201800293

WILEY-VCH

Entry for the Table of Contents (Please choose one layout)

COMMUNICATION

Turn bane into a boon: A unique class of two-photon dyes with anti-solvatochromic fluorescence, optically tunable groups, high fluorescence quantum yields and large two-photon action cross sections in water were developed. They are expected to be useful fluorophore scaffolds in the development of new two-photon probes for bioimaging.

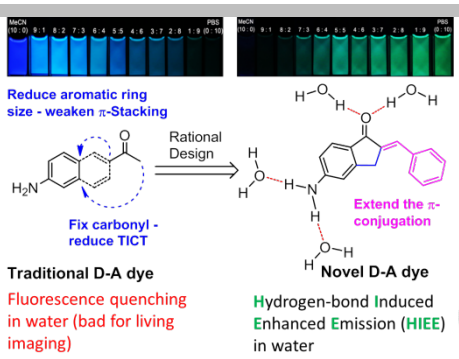

*Tian-Bing Ren, [▽] Wang Xu, [▽] Qian-Ling Zhang, Xing-Xing Zhang, Si-Yu Wen, Hai-Bo Yi, Lin Yuan, * Xiao-Bing Zhang*

Page No. – Page No.

Harvesting Hydrogen Bond Network: Enhance the Anti-Solvatochromic Two-Photon Fluorescence for Cirrhosis Imaging